applied sciences

MDPI

Article

Investigation of Yarrow Essential Oil Composition and Microencapsulation by Complex Coacervation Technology

István Székely-Szentmiklósi [1], Emőke Margit Rédai [2], Béla Kovács [3], Attila-Levente Gergely [4], Csilla Albert [5], Zoltán-István Szabó [1], Blanka Székely-Szentmiklósi [6,*] and Emese Sipos [1]

1 Department of Industrial Pharmacy and Pharmaceutical Management, Specialty Pharmaceutical Sciences, "George Emil Palade" University of Medicine, Pharmacy, Science and Technology of Târgu Mureș, 540142 Târgu Mureș, Romania; istvan.szekely-szentmiklosi@umfst.ro (I.S.-S.); emese.sipos@umfst.ro (E.S.)
2 Department of Pharmaceutical Technology and Cosmetology, Specialty Pharmaceutical Sciences, "George Emil Palade" University of Medicine, Pharmacy, Science and Technology of Târgu Mureș, 540142 Târgu Mureș, Romania; emoke.redai@umfst.ro
3 Department of Pharmaceutical Biochemistry and the Chemistry of Environmental Factors, Fundamental Pharmaceutical Sciences, "George Emil Palade" University of Medicine, Pharmacy, Science and Technology of Târgu Mureș, 540142 Târgu Mureș, Romania; bela.kovacs@umfst.ro
4 Department of Mechanical Engineering, Sapientia Hungarian University of Transylvania, 547367 Târgu Mureș, Romania; agergely@ms.sapientia.ro
5 Department of Food Science, Sapientia Hungarian University of Transylvania, 530104 Miercurea Ciuc, Romania; albertcsilla@uni.sapientia.ro
6 Department of Pharmaceutical Chemistry, Specialty Pharmaceutical Sciences, "George Emil Palade" University of Medicine, Pharmacy, Science and Technology of Târgu Mureș, 540142 Târgu Mureș, Romania
* Correspondence: blanka.szekely-szentmiklosi@umfst.ro

Abstract: Yarrow (*Achillea millefolium* L., AM) is a widely used medicinal plant, with its essential oil highly valued in the cosmetic industry. In view of the numerous biological effects, however, microencapsulation, due to its ability to protect sensitive constituents, transform liquids into solid-state material, and provide modification of release kinetics, might open up new possibilities for the biomedical utilization of yarrow essential oil (AMO). In the current work, yarrow plantation was established by its propagation from spontaneous flora. Following the steam distillation of aerial parts, the chemical composition of the essential oil was determined by GC-MS analysis and compared with two commercial samples. This study concludes that *Achillea millefolium* L. from this region, given the environmental conditions, produces high-azulene-content essential oil. Furthermore, microencapsulation of AMO was successfully performed by complex coacervation into gelatin (GE) and gum arabic (GA) based core–shell microcapsules (MCs). According to the optical microscopic investigation, the particle sizes of the formed polynucleated microcapsules ranged from 14 to 132 µm, with an average of 47 µm. The assessment of morphology by SEM analysis of the freeze-dried form revealed a sponge-like character with embedded circular structures. The microencapsulation was confirmed by FT-IR spectroscopy and differential scanning calorimetry (DSC), while an encapsulation efficiency of 87.6% was determined by UV spectroscopy. GC-MS analysis revealed that microencapsulation preserves the key components of the essential oil. It was concluded that AMO can be effectively processed by complex coacervation followed by freeze-drying into solid-state material for new applications.

Keywords: microencapsulation; complex coacervation; essential oil; *Achillea millefolium* L.

Citation: Székely-Szentmiklósi, I.; Rédai, E.M.; Kovács, B.; Gergely, A.-L.; Albert, C.; Szabó, Z.-I.; Székely-Szentmiklósi, B.; Sipos, E. Investigation of Yarrow Essential Oil Composition and Microencapsulation by Complex Coacervation Technology. *Appl. Sci.* **2024**, *14*, 7867. https://doi.org/10.3390/app14177867

Academic Editor: Marco Iammarino

Received: 29 July 2024
Revised: 30 August 2024
Accepted: 2 September 2024
Published: 4 September 2024

1. Introduction

One of the most widespread and widely used medicinal plants worldwide is yarrow, *Achillea millefolium* L. (AM), a perennial shrub belonging to the *Asteraceae* family. The plant extract and essential oil possess numerous pharmacological properties such as antioxidant, antimicrobial, antispasmodic, and antitumor properties [1].

It is generally recognized that the essential oil content of the plant is low, and it may be influenced by harvest time and environmental conditions [1]. Benedek et al. examined 40 commercial *Achillea* samples from different countries and reported essential oil contents ranging from 0.50% to 5.88% with an average value of 2.06% relative to the dry plant material [2,3]. Klindovits et al. reported a peak accumulation level of essential oil in the range of 0.230–0.334 mg/100 g, with the highest values in the white bud phenophase [4]. Similarly, taking into account the essential oil content, Karlová and Petríková identified the beginning of flowering instead of full flowering as the optimal developmental stage and reported 0.5–1.3% essential oil content [5]. According to Orav et al. in their investigation on wild AM populations from Estonia, the highest essential oil content was obtained from the flower head (4 mg/g), approximately ten-fold more than the amount obtained from the stem and two times higher than quantity values obtained from the leaves. In terms of harvest period, July and August were more favorable in comparison to September [6]. Stevanovic et al. reported yields ranging from 0.32 to 1.01% for indigenous populations of yarrow distributed on salt-affected soils in Serbia. The authors emphasized the importance of different chemotypes derived from different genetic structures. Saline soil features did not represent an important influencing factor. Various cultivars of the plant have been developed to increase the essential oil content and to obtain a more favorable essential oil composition, but it is also generally accepted that in the case of AM, the genetic, ontogenetic, and environmental factors are very important for the composition of the essential oil [2,3].

The monograph on *Millefolii herba* by the European Scientific Cooperative on Phytotherapy (ESCOP) mentions the essential oil as a characteristic constituent, with a content between 0.2 and 5.9%, enumerating between components α- and β-pinene, 1,8-cineole, sabinene, camphor, borneol, β-caryophyllene, and germacrene D, as well as proazulene- and non-azulogenic sesquiterpenes of the guaianolide type, chamazulene carboxylic acid, flavonoids (mainly flavone- and flavonol-O-glycosides) and phenolic acids (mainly dicaffeoylquinic acids) [7]. The European Pharmacopoeia 11th edition yarrow (*Millefolii herba*) monograph foresees 2 mL/kg (dried drug) of essential oil and a minimum of 0.02% proazulene, expressed as chamazulene [8]. Formerly, it was considered that the proazulen accumulation in the plant is related to the ploidy of the species and that there are proazulene-free taxons; however, advancements in analytical techniques have since revealed that proazulene accumulation cannot be linked to ploidy [9], as proazulenes have been detected in species previously considered proazulene-free [10]. Azulenes and their derivatives play an important role in many of the therapeutic effects [11].

As sesquiterpene lactones are considered the most important bioactive materials of AM [12], efforts have been directed toward the isolation and identification of new compounds with this type of structure. Mustakerova et al. reported the isolation of three new sesquiterpene lactones [13]. More recently, Li et al. identified seven yet undescribed guaianolide-type sesquiterpene lactones (millefoliumins) and five analogs [14] as well as six yet undescribed germacrene-type sesquiterpene lactones (millefoliumons) and two known analogs [15].

Traditionally, yarrow essential oil is obtained by steam distillation, but novel extraction techniques have also been implemented, such as ultrasound-assisted extraction [16] or supercritical CO_2 extraction [17,18]. Bocevska and Sovová compared the essential oil composition obtained from *Achillea millefolium* L. by hydrodistillation to that obtained by supercritical CO_2 extraction. It was observed that less volatile components were present in higher quantities in the case of CO_2 extraction, while the yield of monoterpenes was higher when hydrodistillation was applied. This phenomenon is caused by the incomplete separation of monoterpenes from gaseous CO_2 [17]. In a recent study, Ivanović et al. evaluated the phytochemical profiles of natural deep eutectic solvent (NADES)-based extracts obtained by ultrasound-assisted extraction with those obtained using conventional solvents: 80% ethanol, 80% methanol, and water. In the case of alcoholic and aqueous extractions, the bioactive compounds, chlorogenic acid, isomers of dicaffeoylquinic acids, and flavonoids were the most abundant bioactive compounds [19]. In n-hexane and

diethyl-ether extracts, Mohammed et al. identified germacrene D, viridiflorol, α-Thujone, β-thujone trans-sabinene hydrate, and 1.8-cineole as major components. In comparison to the distilled material, the extraction process using non-polar solvents resulted in increased amount of higher-molecular-weight volatile compounds, with more sesquiterpenes than monoterpenes [20]. During steam distillation, on the effect of heat and water, the proazulene achillicin is transformed through chamazulenic acid into chamazulene, which confers the characteristic blue color to yarrow essential oil [21]. The yield of distillation was reported to vary based on different factors. Orav et al. investigated the effect of distillation time in the 0.5–3 h interval. The increase in yield along with an increase in the relative amount of chamazulen was reported at prolonged distillation times [6].

The presence of numerous compounds with various biological activities can explain the wide spectrum of pharmacological effects that have been attributed to *Achillea millefolium* L., such as analgesic, anti-inflammatory, antidiabetic, cholagogue, spasmolytic, antitumor, antioxidant, antifungal, and antiseptic activities [22,23]. In traditional European medicine, it is used in the treatment of inflammatory and spasmodic gastro-intestinal complaints and hepato-biliary disorders and as an appetite-enhancing drug [3], but also in menstrual irregularity, to relieve menstrual cramps and pain, and for the healing of wounds and ulcers [24].

According to the European Medicines Agency (EMA)'s herbal monographs on *Achillea millefolium* L.—*herba* and *Achillea millefolium* L.—*flos*, their well-established use could be considered as scientifically proven to treat temporary loss of appetite; mild, spasmodic gastro-intestinal complaints, including bloating and flatulence; treatment of minor spasms associated with menstrual periods; and the treatment of small superficial wounds [25,26].

In the biomedical field, recent research work was directed toward elucidating the anti-inflammatory effects of essential oil [27] and its efficacy in the treatment of peptic ulcers [28] and ulcerative colitis [29]. Ma et al. reported that chondrocytes were protected during chamazulene treatment against IL-1β-induced osteoarthritic inflammation [30]. Csupor et al. described the antitumor potential of the plant [31].

Given the sensitivity of several components of essential oil to environmental conditions [32], appropriate formulation and conditioning are required to prevent degradation and assure the long-term preservation of its specific composition [33]. In many cases, the transformation of essential oil from a liquid state into free-flowing and easily manageable dry powders might be of fundamental importance to fit a specific application [34]. For this purpose, Rakmai et al. encapsulated yarrow essential oil into hydroxypropyl-β-cyclodextrin followed by freeze-drying. Researchers reported enhancements in protection against sunlight but also an increase in the antibacterial activity against *Staphylococcus aureus* and *Escherichia coli* [35]. Ahmadi et al. applied ionic gelation for the nanoencapsulation of Yarrow essential oil using chitosan and sodium tripolyphosphate and thus managed to obtain a sustained-release formulation, which in consequence prolonged the pesticidal property against *Tetranychus urticae* [36]. Microencapsulation is a preferred alternative for preserving the properties of essential oils and enhancing their usability. Although there are numerous examples of such attempts in the literature, studies focusing on yarrow essential oil remain scarce. Despite the emergence of numerous microencapsulation methods over time, complex coacervation remains one of the most commonly used techniques in the food and pharmaceutical industries due to its simplicity and cost-effectiveness [37]. This is an associative phenomenon that occurs between oppositely charged polymers when they interact under suitable conditions in aqueous media, which leads to the formation of a polymer-rich phase and a polymer-poor phase at equilibrium; dispersed droplets become encapsulated if this process results in a reduction in interfacial free energy [38]. Due to its beneficial properties, including biodegradability, low immunogenicity, easy availability, and cost-effectiveness, gelatin (GE) continues to be one of the most commonly used shell materials for microencapsulation [39]. It is frequently combined with gum arabic to create a protein–polysaccharide complex that can effectively protect and deliver encapsulated materials [40–42].

In the current work, we aimed to bring into cultivation the yarrow from the spontaneous flora found in our region, to obtain essential oil by steam distillation, and to evaluate its quality by comparison with commercially available samples by GC-MS analysis. Another goal of this study was to perform the microencapsulation of yarrow essential oil by complex coacervation technology in gelatin (GE)- and gum arabic (GA)-based core–shell microcapsules and to obtain solid-state material by freeze-drying, as well as to characterize microcapsules (MCs) and the enclosed essential oil. This involved macroscopic and microscopic investigation of coacervates and solid microcapsules, assessing their physicochemical properties by FT-IR and DSC analysis, and determination of encapsulation efficiency and loading capacity by UV spectroscopy. The GC-MS investigation of microcapsules also reveals their efficiency in preserving the essential oil, as well as their suitability for potential applications in various industries.

2. Materials and Methods

2.1. Biomaterial

Achillea millefolium L. (AM) was cultivated in Romania, Transylvania Region, Mureș County, near the village of Dumbrăvioara located in the floodplain of Mureș River, situated at 46°38′ latitude, 24°38′ longitude, and 336 m elevation. The aerial parts, which were subjected to steam distillation, were harvested in 2021 and 2022.

2.2. Yarrow Essential Oil

The yarrow essential oil (AMO) was obtained by steam distillation of the aerial parts of the plant on a glassware laboratory-scale steam distillation set with a bioreservoire of 2 L capacity, a Graham-type condenser, and a separation vessel. Biomaterial was collected during the full bloom period at the end of June. Between 400 and 450 g of fresh herb was introduced in the bioreservoire and 1500 g of water was used for steam generation. The steam distillation process was performed for 2.5 h. Five consecutive runs were completed. Distilled oil was separated by using a separation funnel. The essential oil yield percentages were 0.068% in 2021 and 0.070% in 2022.

Due to the limited quantity of biomaterial derived from a relatively small cultivation area along with the low yield of the steam distillation process, the microencapsulation had to be performed by using commercially available yarrow essential oil. For this reason, *Achillea millefolium* L. essential oils from Bulgarian and Romanian markets were purchased, from Essences, JPV Middendorf Ltd., Nikolovo, Bulgaria and Oleya, SC Cream Apothecary SRL, Bucșani, Romania, respectively.

2.3. Shell Materials

Gelatin type A of porcine origin with a gel strength of approx. 175 Bloom value was purchased from Sigma Aldrich (St. Louis, MO, USA). Gum arabic from acacia trees was purchased from Sigma Aldrich Chemie (Steinheim, Germany).

Hydrochloric acid was purchased from Silal Trading SRL (Bucharest, Romania) and used at a 0.5 N concentration for pH adjustment.

Glycerol as a crosslinker was purchased from Chimreactiv SRL (Bucharest, Romania).

2.4. Chemicals

All chemicals used were of analytical grade: n-Hexane for liquid chromatography LiChrosolv® (Merck, Darmstadt, Germany), ethanol (gradient-grade) for liquid chromatography LiChrosolv® (Merck, Darmstadt, Germany), and hydrochloric acid 37% (Silal Trading SRL, Bucuresti, Romania).

2.5. Microencapsulation Method

Complex coacervation technology was applied according to the following major steps: 50 g of 3% *w*/*w* gum arabic (GA) aqueous solution was prepared by dissolving gum arabic at room temperature under continuous stirring by the means of a magnetic stirrer (Arec,

Velp Scientifica, Usmate, Italy) at 800 rpm. Fifty grams of 3% gelatin (GE) aqueous solution was prepared under continuous stirring and concomitant heating up to 50 ± 2 °C using a magnetic stirrer at 800 rpm. Gelatin type A with a gel strength of approx. 175 Bloom was used; 2.7 g of yarrow essential oil was emulsified into the formerly prepared 3% *w*/*w* gelatin solution by using an IKA DI 18 B type ultraturrax (IKA®-Werke GmbH & Co. KG, Staufen, Germany) equipped with an IKA S 18 N–19 G type dispersion tool (IKA®-Werke GmbH & Co. KG, Staufen, Germany) for 10 min at a rotation speed of ≈ 5000 rpm. This emulsion was added to the formerly prepared aqueous gum arabic solution under continuous stirring. At addition, the temperature of both components was in the interval of 50 ± 2 °C. The pH adjustment to pH = 4.0 ± 0.05 of the mixture was made by using 0.5 N HCl. After gradual cooling to 10 °C in an ice bath, the crosslinking agent glycerol (1 g) was added to harden the formed shell. Separation and purification of microcapsules were performed by decantation and washing with purified water twice (volume 2 × 50 mL). After decantation, 50 mL of water was added to the microcapsule slurry and the mixture was stirred by the means of a magnetic stirrer for 15 min. The washing procedure was repeated two times (Figure 1).

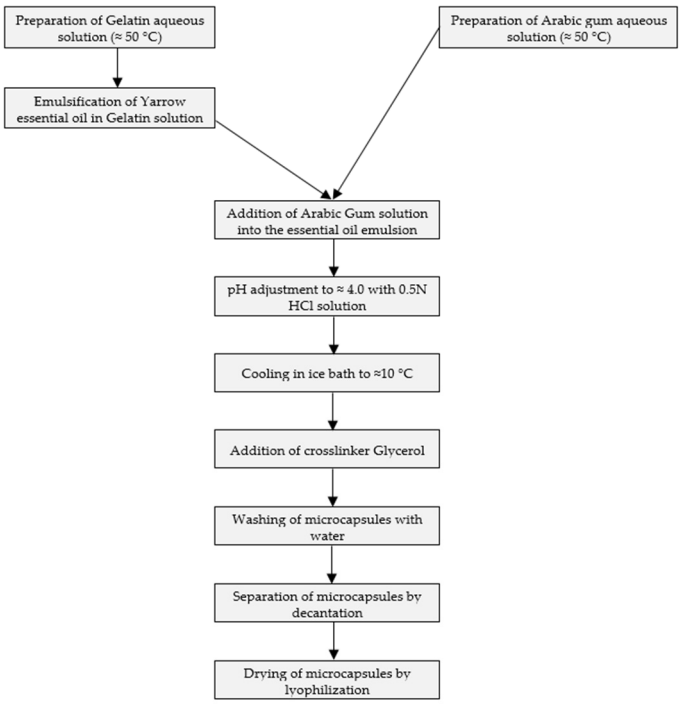

Figure 1. Process steps of yarrow essential oil microcapsule formation.

Simultaneously, microcapsules without essential oil, referred to as placebo (PL), were produced using the aforementioned method. The schematic process of obtaining microcapsules is presented in the flow chart (Figure 1).

2.6. Freeze-Drying

Freeze-drying of microcapsules was performed in a Biobase BK FD10S (Biobase, Jinan, China) instrument by applying 4 h of freezing at −55 °C followed by 20 h of drying under a vacuum of 10 Pa.

2.7. Optical Microscopic Investigation

The optical microscopic investigation was performed on an Optika B-150D-BRPL brightfield microscope (Optika SRL, Ponteranica, Italy) equipped with an integrated 3.1 MP camera at magnifications of 40× 100×, 400×, and 1000×. For particle size measurement, Optika Proview 2020 software (Optika SRL, Ponteranica, Italy) was used. Microscopic specimens were prepared by placing one droplet of microcapsule dispersion on a glass

slide, after which a cover slip was gently applied. In the case of the 1000× magnification, immersion oil was applied on the top of the cover slip.

2.8. SEM Investigation

The morphology of the obtained products was investigated by scanning electron microscopic (SEM) imaging, with the use of a JEOL JSM-5200 scanning electron microscope (JEOL, Tokyo, Japan) at 10 kV potential. The samples were used as is (without sputter coating) and were fixed by conductive carbon adhesive tape.

2.9. FT-IR Spectroscopy

FT-IR spectroscopy of solid samples was performed on a Bruker Tensor 27 IR spectrophotometer (Bruker Optics, Ettlingen, Germany) controlled by the Opus software (version 7.2). IR spectra of the solid components, the physical mixture, and the prepared products were recorded using KBr (Sigma Aldrich, Merck, Darmstadt, Germany) pellets, in transmittance mode over the 400–4000 cm^{-1} wavenumber range. The sample to KBr ratio was 1:100. Each sample was scanned 16 times, with a resolution of 2 cm^{-1}.

FT-IR spectroscopy of essential oil was performed on a Nicolet 380 IR spectrophotometer (Thermo Electron Corporation, Madison, WI, USA) controlled by the OMNIC 8.0 software.

2.10. Differential Scanning Calorimetry (DSC)

The thermal behaviors of GE, GA, and lyophilized microcapsules were analyzed using a Differential Scanning Calorimeter (DSC-60, Shimadzu Corporation, Kyoto, Japan). For each sample, 3–5 mg was placed in an aluminum pan, with an empty sealed pan as a reference. DSC analysis was carried out at a heating rate of 10 °C/min over a temperature range from 30 to 300 °C.

2.11. Visible Spectroscopic Analyses

Visible spectroscopic determinations were performed on a Shimadzu UV-1800 spectrophotometer (Shimadzu Co., Kyoto, Japan), controlled by UVProbe Software, using cuvettes made of special quartz glass with an optical path length of 10 mm (Hellma Analytics, Müllheim, Germany).

2.11.1. Qualitative Analyses

The essential oil described in Section 2.2. was compared with two commercially available essential oils purchased from the Bulgarian and Romanian markets by UV-VIS spectra of their 10 mg/mL alcoholic solutions. The wavelength ranges used for all samples were 400–800 nm.

2.11.2. Quantitative Analyses

Yarrow essential oil content in the microcapsules was determined by the visible spectroscopic method and quantified through the calculation of encapsulation efficiency and loading capacity.

The method was adapted with minor modifications from a similar spectrophotometric technique involving ethanol, as described by Gonçalves et al. [42]. The amount of essential oil in microcapsules was measured using the following steps: firstly, 50 mg of microcapsules was powdered in a mortar; 10 mL of absolute alcohol was added and magnetically stirred for 10 min to dissolve the total quantity of essential oil. Then, another 50 mg of microcapsules was weighed and stirred magnetically for 10 min with 10 mL of absolute alcohol, and the supernatant was collected to recover the AMO found on the surface of the microcapsules. The alcoholic solutions were filtered and assayed spectrophotometrically at 603 nm, after appropriate dilution. The AMO concentrations were calculated using a calibration curve built in the concentration range of 1–10 mg/mL.

The encapsulation efficiency (EE) and loading capacity (LC) were calculated according to the following equations:

$$EE = m_m / m_o \cdot 100 \quad (1)$$

where m_m is the amount (mg) of oil contained in the microcapsules and m_o is the initial oil amount (mg) used. The amount of oil in microcapsules is determined by the difference between the total oil content (m_{to}) and the surface oil content (m_{so}):

$$m_m = m_{to} - m_{so} \quad (2)$$

$$LC = m_m / M \cdot 100 \quad (3)$$

where M is the total amount (mg) of microcapsules [40,43].

2.12. GC—MS Investigation

The method was adapted with minor modifications from a similar gas chromatography technique applied in a case of essential oil analysis by Khan et al. [44]. GC–MS analysis of the essential oil was performed on an Agilent single-quadrupole mass spectrometer with an inert mass selective detector (MSD-5977 A, Agilent Technologies, Santa Clara, CA, USA). This was directly connected to an Agilent 7890B gas chromatograph equipped with a split–splitless injector, a quick-swap assembly, an Agilent 7693 autosampler, and an HP-5MS fused silica capillary column (5% phenyl 95% dimethylpolysiloxane, 30 m × 0.25 mm i.d., 0.25 µm film thickness, Agilent Technologies, USA). The HP-5MS column was operated with an injector temperature of 250 °C. The oven temperature profile included an isothermal hold at 50 °C for 4 min, a ramp of 4 °C/min to 220 °C, and an isothermal hold for 2 min, followed by a second ramp to 280 °C at 20 °C/min and a final isothermal hold for 15 min.

Before analysis, the essential oil was dissolved in hexane (1/100, *v*/*v*). For microcapsules, extraction of essential oil was performed from 500 mg using 1 mL of hexane followed by filtration. Next, 1 µL of the solution was injected in 1:10 split mode. Helium was used as the carrier gas at a flow rate of 1 mL/min. GC–TIC profiles and mass spectra were obtained using the MSD ChemStation software, version F.01.01.2317 (Agilent). All mass spectra were acquired in the EI mode (scan range of *m*/*z* 45–600 and ionization energy of 70 eV). The electronic-impact ion source and the MS quadrupole temperatures were set at 230 °C and 150 °C, respectively, with the MSD transfer line maintained at 280 °C. Mass spectra were identified with NIST 14 Mass Spectral Library.

3. Results and Discussion

3.1. Chemical Composition of Yarrow Essential Oils

3.1.1. Chemical Composition of Self-Prepared Yarrow Essential Oils

Yarrow essential oil compositions obtained in two consecutive years (2021 and 2022) were determined by GC-MS analyses. Obtained results are presented in Table 1.

In yarrow essential oil obtained in the year 2021, 43 compounds were identified, while in the case of that obtained in the year 2022, 37 compounds were identified by GC-MS analyses. In both cases, the essential oil was characterized by high chamazulene, germacrene D, and caryophyllene content, and the same six compounds were in the highest quantity. The order of the major compounds according to their amount was the same in the essential oils obtained in two consecutive years. Germacrane D, eucalyptol, and caryophyllene oxide were almost in the same quantities. Higher variation was noticed in the level of chamazulene, caryophyllene, and β-pinene. While caryophyllene was present in a higher quantity in the case of essential oil obtained in 2021, the essential oil obtained in 2022 contained higher amounts of chamazulene and β-pinene.

According to the GC-MS determination, the major constituents of *Achillea millefolium* L. essential oils were as presented in Figure 2.

Table 1. Composition of yarrow essential oil obtained in two consecutive years.

No.	Component	Obtained in 2021 %	Obtained in 2022 %	No.	Component	Obtained in 2021 %	Obtained in 2022 %
1.	alpha-pinene	0.64	0.85	24.	**caryophyllene**	**16.39**	**12.88**
2.	**beta pinene**	**6.10**	**12.45**	25.	beta copaene	0.29	0.26
3.	beta myrcene	0.11	0.14	26.	humulene	2.56	1.99
4.	4-carene	0.11	0.09	27.	cis beta farnesene	0.14	-
5.	o-cymene	0.13	0.23	28.	**germacrene D**	**21.28**	**21.13**
6.	beta terpinene	-	0.47	29.	beta selinene	-	0.16
7.	**eucalyptol**	**3.38**	**3.81**	30.	bicyclo germacrene	2.08	1.62
8.	trans beta ocimene	0.13	0.49	31.	alpha muurolene	0.21	0.13
9.	beta ocimene	0.15	0.40	32.	alpha farnesene	0.16	-
10.	gamma terpinene	0.49	0.38	33.	gamma muurolene	0.42	0.27
11.	linalool	0.45	0.13	34.	cadinene	1.04	0.64
12.	alpha campholenal	-	0.29	35.	nerolidol	0.61	0.14
13.	pinocarveol	0.25	0.23	36.	aromadendrane	0.52	0.75
14.	camphor	0.11	0.15	37.	**caryophyllene oxide**	**3.02**	**3.38**
15.	pinocarvone	0.78	1.13	38.	valerena-4,7(11)-diene	0.35	-
16.	terpinen-4-ol	0.49	-	39.	alpha elemene	0.22	-
17.	alpha terpineol	1.05	0.43	40.	alloaromadendrene	0.17	0.1
18.	3-carene	1.16	0.29	41.	tau cadinol	0.53	0.42
19.	lavandulyl propionate	0.22	-	42.	alpha cadinol	0.36	0.47
20.	eugenol	0.13	-	43.	**chamazulene**	**21.97**	**25.37**
21.	gamma limonene	0.68	-	44.	homosalate	0.14	-
22.	alfa copaene	0.21	0.29	45.	geranil alpha terpinene	0.43	1.45
23.	beta bourbonene	0.45	2.09	46.	trans alpha bergamotene	0.23	0.59
					Total identified	**90.34**	**96.09**

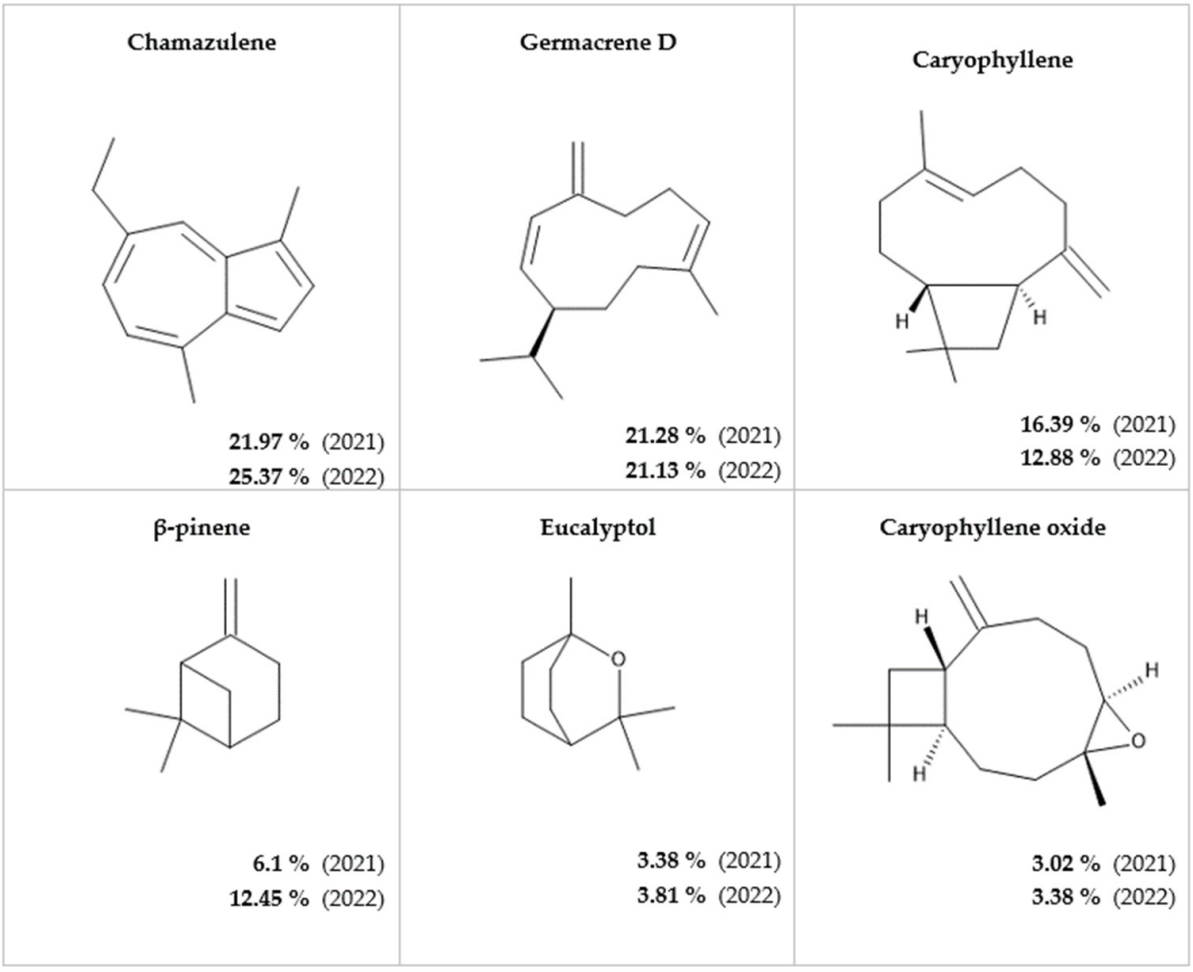

Figure 2. Major components of *Achillea millefolium* L. essential oil obtained by steam distillation in two consecutive years.

3.1.2. Comparison of Yarrow Essential Oils of Different Origins

Due to the lack of specific regulation on quality, it was proposed to compare the obtained composition with commercially available essential oils. For this reason, two samples were purchased, one from the Romanian market and the other one from the Bulgarian market. Considering the blue color conferred by azulene content, the aspect of yarrow essential oil might serve as a first sign of the composition and quality of different origins. Figure 3b intends to illustrate the encountered color differences of yarrow essential oils from different origins.

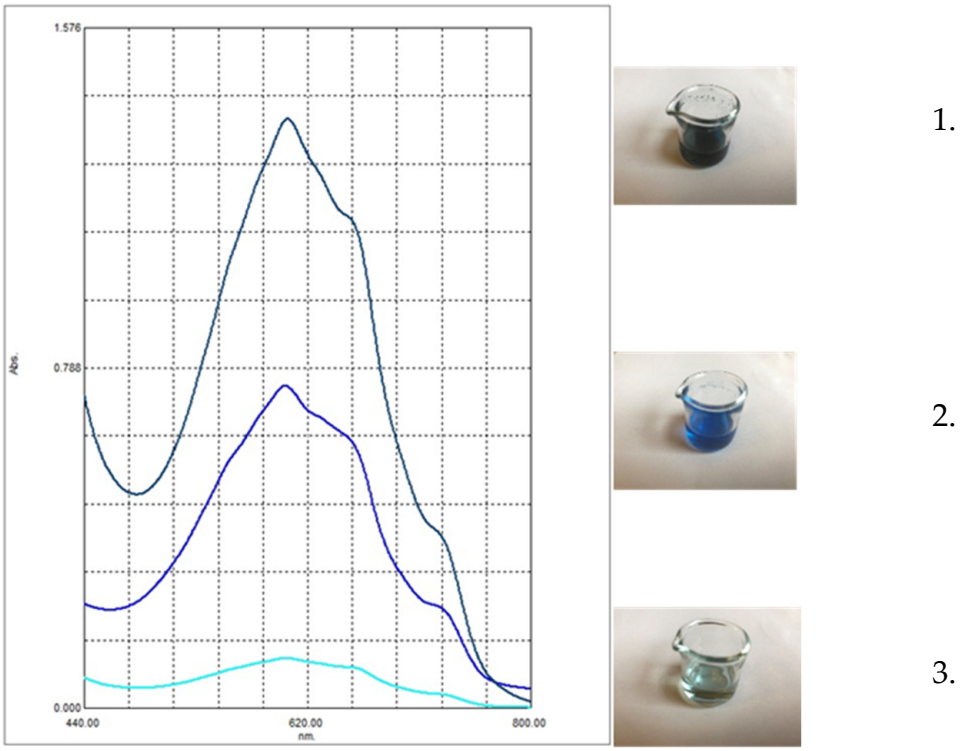

Figure 3. Comparison of yarrow essential oils. (**a**) UV-VIS spectra of alcoholic solutions of yarrow essential oils of different origins; (**b**) visual aspect of yarrow essential oils obtained by steam distillation: 1. self-prepared, 2. from Bulgaria, 3. from Romania. The color and order of the curves (**a**) match the color and order of the solutions ((**b**) 1, 2, 3 from top to bottom).

In Figure 3b, it can be observed that in the case of our essential oil and the commercial sample of Bulgarian origin, the blue color is predominant, while in the case of the purchased oil originating from the Romanian market, the color of the oil is more greenish. The observed difference is also reflected in the UV-VIS spectra of the essential oils in alcoholic solution, presented in Figure 3. The highest peaks achieved at the specific absorption wavelength of chamazulen (603 nm) were registered in the case of our essential oil. In the case of the oil of Bulgarian origin, lower peak intensity was obtained, while the yarrow oil of Romanian origin resulted in the lowest peak. The maximum wavelength is consistent with the value provided in the European Pharmacopoeia, which specifies the measurement of chamazulene content in xylene solution at 608 nm [8].

Furthermore, the purchased essential oils were also characterized by GC-MS analysis. The results obtained are presented in Table 2.

In the yarrow essential oil purchased from the Bulgarian market, 45 components were identified. The major constituents were beta-pinene, sabinene, camphor, caryophyllene and linalool. Germacrene D and chamazulene were present in only 6.1% and 3.8%, respectively.

Table 3 contains the composition of yarrow essential oil purchased from the Romanian market.

Table 2. Components of yarrow essential oil commercial sample purchased from Bulgarian market.

No.	Compound [1]	AMO Peak% (Bulgarian Market)	No.	Compound [1]	AMO Peak% (Bulgarian Market)
1.	thujene	1.08	24.	D-carvone	0.60
2.	alpha pinene	4.47	25.	**piperitone**	**5.85**
3.	camphene	0.60	26.	sabinil acetate trans	0.32
4.	**sabinene**	**8.31**	27.	bornyl acetate	2.68
5.	**beta pinene**	**8.59**	28.	thymol	1.31
6.	beta myrcene	0.41	29.	diosphenol	0.40
7.	alpha terpinene	0.47	30.	carvacrol	1.41
8.	p cymene	1.55	31.	piperitenone	0.52
9.	D limonene	2.14	32.	4-Acetyl-1-methylcyclohexene	1.86
10.	**eucalyptol**	**5.09**	33.	beta bourbonene	0.76
11.	gamma terpinene	2.18	34.	beta elemene	0.54
12.	artemisia keton	1.93	35.	**caryophyllene**	**7.74**
13.	terpinolene	0.32	36.	humulene	1.57
14.	**linalool**	**6.78**	37.	beta farnesene	1.07
15.	alpha thujone	2.84	38.	gamma muurolene	0.28
16.	beta thujone	0.46	39.	**germacrene D**	**6.10**
17.	**2-bornanone (camphor)**	**7.84**	40.	trans alpha bergamotene	0.63
18.	1-menthone	0.27	41.	cis-γ-Bisabolene	0.38
19.	endo borneol	1.77	42.	cadinene	0.79
20.	terpinen 4-ol	1.66	43.	caryophyllene oxide	1.09
21.	alpha terpineol	0.42	44.	bisabolon oxide A	0.20
22.	cis dihydrocarvone	0.56	45.	**chamazulene**	3.80
23.	pulegone	0.30		**Total identified**	**99.94%**

[1] In order of retention time.

Table 3. Components of yarrow essential oil commercial sample purchased from Romanian market.

No.	Compound [1]	AMO Peak% (Romanian Market)
1.	thujene	0.08
2.	**alpha pinene**	**17.93**
3.	camphene	0.36
4.	sabinene	2.82
5.	beta-pinene	2.76
6.	beta myrcene	1.47
7.	p-cymene	0.15
8.	limonene	3.34
9.	**1,8 cineole**	**7.37**
10.	gamma terpinene	0.07
11.	**fenchone**	**27.22**
12.	linalool	2.57
13.	alpha thujone	2.99
14.	beta-thujone	0.42
15.	terpinen-4-ol	0.12
16.	geraniol	2.29
17.	beta bourbonene	0.06
18.	beta farnesene	4.48
19.	germacrene D	0.39
20.	gamma elemene	0.23
21.	gamma cadinene	0.10
22.	delta cadinene	0.11
23.	spathulenol	0.25
24.	tau cadinol	0.30
25.	bisabolol oxide B	2.26
26.	bisabolon oxide A;	2.43
27.	chamazulene	0.46
28.	**estragole**	**15.36**
	Total identified	**98.39%**

[1] In order of retention time.

In the case of yarrow essential oil purchased from the Romanian market, fenchone, alpha-pinene, estragole, and 1,8-cineole were the four major components. Chamazulen was detected in only 0.46%. The chamazulene content of essential oils analyzed was in good correlation with their observed colors (Figure 3).

The table below (Table 4) summarizes data from the literature on the composition of yarrow essential oil, highlighting the five most abundant components identified.

Table 4. Major components of yarrow essential oils from different studies.

Country/ Region	The Five Most Abundant Components Identified in Yarrow Essential Oil (Relative Amount)					Yield	Authors	Refs.
Romania (western part)	chamazulene (38.89%)	germacrene D (12.90%)	β-caryophyllene (11.52%)	β-pinene (10.66%)	n.d.*	0.47%	Jianu et al.	[45]
Romania (north-western)	Flowers						Costescu et al.	[46]
	β-pinene (17.2%)	chamazulene (12.9%)	β-phellandrene (12.1%)	1,8-cineole (6.8%)	β-caryophyllene (6.0%)	0.5%		
	Leaves							
	α-bisabolol (16.0%)	β-pinene (9.9%)	chamazulene (9.7%)	β-phellandrene (8.0%)	1,8-cineole (7.7%)	0.7%		
	Root							
	chamazulene (33.82%)	α-bisabolol (10.27%)	β-caryophyllene (5.04%)	caryophyllene oxide (4.43%)	β -pinene (4.2%)	0.9%		
	Stem							
	chamazulene (45.79%)	β-caryophyllene (7.67%)	β-cubebene (5.6%)	ledol (3.24%)	β-phellandrene (3.18%)	1.2%		
Egypt (west of Nile delta)	β-pinene (24.1–54.6%)	chamazulene (10.1–26.7%)	germacrene D (1.3–10.3%)	β-caryophyllene (11.52%)	limonene (6.4–11.9%)	0.067–0.186%	Aziz et al.	[1]
Turkey (Eastern Anatolia)	1,8-cineole (75.19%)	α-phellandrene (5.53%)	p-eugenol (5.53%)	camphor (5.45%)	α-terpineol (2.09%)	n.d.*	Yildirim et al.	[47]
Iran (El.: 1339 m, Lat. east: 33.638, Long. n	borneol (20.14–36.35%)	thymol (10.01–10.14%)	carvacrol (8.14–10.14%)	α-pinene (6.45–7.45%)	camphene (2.14–4.65%)	1.54% *v*/*w*, 2.01% *v*/*w*	Abdossi and Kazemi	[48]
Iran (West Azerbaijan Province)	1,8-cineole (21.28–34.51%)	camphor (7.27–14.07%)	chamazulene (4.18–11.34%)	α-eudesmol (2.09–9.63%)	α-cadinol (2.35–7.73%)	0.14–0.24% *v*/*w*	Farhadi et al.	[49]
Portugal (Lisbon botanical garden)	Flowers						Figueiredo et al.	[50]
	1,8-cineole (28.7%)	sabinene (15.4%)	terpinene-4-ol (3.4%)	camphor (3.3%)	γ-terpinene (3.2%)	0.2% *v*/*w*		
	Leaves during flowering							
	1,8-cineole (24.5%)	trans-sabinene hydrate (10.2%)	germacrene D (7.2%)	terpinene-4-ol (5.6%)	sabinene (5.4%)	0.2% *v*/*w*		
	Leaves during vegetative period							
	germacrene D (65.1%)	α-farnesene (12.0%)	δ-elemene (4.6%)	bicyclogermacrene (3.7%)	β-caryophyllene (2.1%)	0.1% *v*/*w*		
Serbia (southern part)	1,8-cineole (28.8%)	camphor (11.0%)	borneol (5.9%)	β-pinene (5.4%)	caryophyllene oxide (3.3%)	n.d.*	Smelcerovic et al.	[10]
Brazil (Umuarama, Parana State)	α-farnesene (31.66%)	chamazulene (17.17%)	β-caryophyllene (10.27%)	sabinene (8.77%)	bicyclo-germacrene (5.84%)	0.4%	Daniel et al.	[51]
Estonia	β-pinene (14.9–29.2%)	1,8-cineole (6.9–18.3%)	sabinene (2.9–17.6%)	chamazulene (0.1–12.7%)	guaiol (0.3–11.8%)	2–4 mg/g	Orav et al.	[6]
India (subtropical region)	germacrene D (1.1–46.6%)	sabinene (4.0–38.9%)	borneol (4.7–24.9%)	camphor (0.6–17.6%)	α-pinene (0.8–11.7%)	0.10–0.70%	Verma et al.	[52]
Serbia (saline habitats: northern parts—Vojvodina province)	trans-chrysanthenyl acetate (5.84–21.33%)	chamazulene (1.51–15.84%)	lavandulyl acetate (0.90–14.88%)	trans-caryophyllene (7.57–9.53%)	β-pinene (3.18–8.89%)	0.32–1.01%	Stevanovic et al.	[2]

Table 4. *Cont.*

Country/ Region	The Five Most Abundant Components Identified in Yarrow Essential Oil (Relative Amount)					Yield	Authors	Refs.
Poland (south eastern part)	Flowers β-pinene (12.22%)	(E)-nerolidol (7.34%)	1,8-cineole (6.45%)	sabinene (6.04%)	camphor (5.28%)	0.598%	Konarska et al.	[53]
	Herb β-pinene (9.90%)	bornyl acetate (9.23%)	borneol (6.18%)	1,8-cineole (5.83%)	camphor (5.81%)	0.235%		
France (Midi-Pyrenees region Toulouse)	camphor (12.8%)	germacrene D (12.0%)	(E)–nerolidol (7.3%)	sabinene (6.7%)	(E)-p-metha-2,8-dien-1-ol (4.5%)	0.07% (raported to fresh weight)	El-Kalamouni et al.	[54]
Saudi Arabia	Stems α-Thujone (29.54%)	β-Thujone (18.05%)	1,8-cineole (14.19%)		Trans-sabinene hydrate (3.70%)	0.33%	Mohammed et al.	[20]
	Leaves α-Thujone (37.02%)	β-Thujone (21.58%)	1,8-cineole (13.90%)	Trans-sabinene hydrate (8.29%)	Thymol (3.51%)	0.65%		
	Herb α-Thujone (23.59%)	Germacrene D (14.73)	β-Thujone (14.70%)	Viridiflorol (10.62%)	1,8-cineole (8.29%)	0.61%		

* n.d.—no data.

The data in Table 4 reveal that the composition of yarrow essential oil is very diverse, and it is greatly influenced by the type of plant material and its place of origin. The highest chamazulene content was measured in stem samples from Romania, exceeding 45%. The germacrene D content was highest (65%) in yarrow leaves from Portugal during full bloom. Caryophyllene was found in the greatest quantity (11.5%) in yarrow essential oils from Romania and Egypt. Regarding other components, essential oils have a very diverse composition. In many oils, 1,8-cineole leads with a significant percentage, ranging from 21.28% to 34.51%, but there is also an exceptionally high value reported in the literature, measured as the main component in the essential oil from Turkey, at 75%. In some samples, beta-pinene is present in larger quantities, while in other essential oils, alpha-farnesene is predominant. The ratio of main components found in the self-prepared yarrow essential oil is consistent with the composition reported for the essential oil from western Romania, while the one purchased from Bulgaria contains beta-pinene, sabinene, camphor, caryophyllene, linalool, and germacrene D as main components in amounts greater than 5%. Among these, sabinene and camphor are characteristic components of certain essential oils; linalool is not listed as a main component in the literature but is present in smaller amounts in both our samples and those purchased from the Romanian market.

As far as the yield is concerned, our results align with those obtained by El-Kalamouni et al. [54] on distilling fresh material originating from the Midi-Pyrenees region of France. Taking into account yields reported for distillations of dried biomaterial, these generally ranged between 0.1 and 0.7%, rarely exceeding 1%.

3.2. Macroscopic and Microscopic Investigation of Complex Coacervate Formation

3.2.1. Macroscopic Aspect of Coacervates

The yarrow essential oil-loaded microcapsules were prepared using gelatin and gum arabic solution, with the complex coacervation method. The formation of microcapsules was achieved by the addition of essential oil emulsion obtained in gelatin solution to gum arabic aqueous solution, followed by pH adjustment, consecutive cooling, and crosslinking with glycerol. Solutions were kept stirring during the complete technological process. Special attention was paid to the cooling phase, as in previous optimization experiments, it was observed that an abrupt temperature decrease might result in the formation of an agglomerate instead of microcapsules.

The macroscopic aspect of the microcapsule sediment is presented in Figure 4.

Figure 4. Yarrow essential oil microcapsule sediment.

3.2.2. Microscopic Aspect of Coacervates

The preparation of the microcapsules was tracked using optical microscopy imaging, captured at different magnification levels (40×, 100×, 400×, and 1000×). Samples for microscopic investigations were taken during the third washing cycle from the microcapsule dispersion. From the lower magnifications (40×, 100×), it could be observed that polydisperse circular-shaped microcapsules were formed with diameters in the range of 14–132 µm. On images recorded at higher magnifications (400×, 1000×), it could be noticed that microcapsules have a polynucleated core, which is formed from essential oil droplets accumulated in the center of the microcapsules, and there is a narrow droplet-free layer surrounding the interior wall of the microcapsules. The optical microscopic investigations of microcapsules are presented in Figure 5.

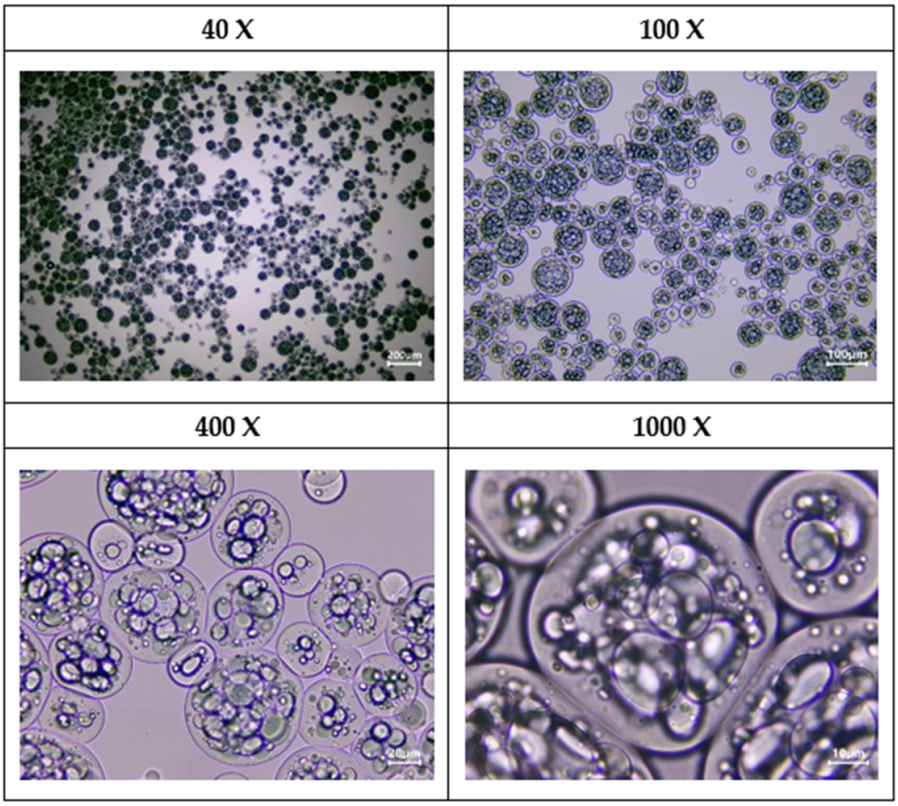

Figure 5. Optical microscopic images of yarrow essential oil containing microcapsules at different magnifications.

The particle size characteristics are presented in Table 5.

Table 5. Particle size characterization of the obtained yarrow essential oil-loaded microcapsules.

Particle Size (μm)			SD	RSD%	Median (μm)	Polydispersity Index
Average [1]	Min.	Max.				
47	14	132	20.71	44.31	42	0.20

[1] n = 305.

These morphological characteristics were also observed by Comunian T. et al. when they produced microcapsules of ascorbic acid through complex coacervation using gelatin and gum arabic [55]. According to Alvim and Grosso, the diameters of moist particles ranged between 43.7 ± 3.4 and 96.4 ± 10.3 μm when these authors produced microcapsules of paprika oleoresin by complex coacervation using similar encapsulating agents [56].

3.3. Macroscopic and Microscopic Investigation of Solid Microcapsules

3.3.1. Macroscopic Aspect of Microcapsules

After three consecutive washing and decantation cycles, the separated microcapsule slurry was freeze-dried and a blue-colored material with a loose structure was obtained. Figure 6 shows the aspect of the freeze-dried microcapsules.

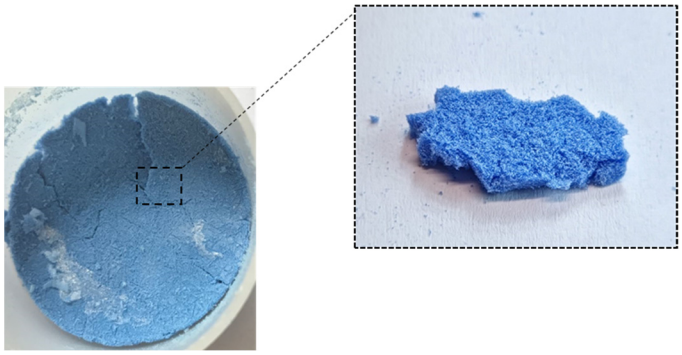

Figure 6. Macroscopic aspect of freeze-dried microcapsules.

3.3.2. Microscopic Aspect of Microcapsules

The loose, sponge-like structure is also reflected in the SEM image of the freeze-dried microcapsules (Figure 7). The spongious matrix is formed by numerous embedded spherical structures, which represent the individual lyophilized microcapsules interconnected by solid bridges.

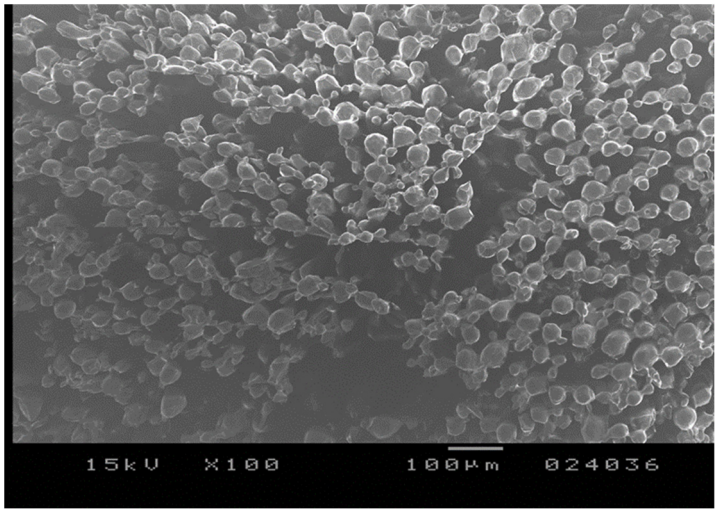

Figure 7. Assessment of morphology by SEM.

Similar phenomena of solid bridge formation and aspects were described by the authors T.A. Comunian et al. [55], Alvim and Grosso [56], and Saravanan and Panduranga Rao, who produced coacervated pectin–gelatin and alginate–gelatin microcapsules [57]. Rocha-Selmi et al. also observed this structure when aspartame was microencapsulated using double emulsion followed by complex coacervation with gelatin and gum arabic [58].

Despite the bonding observed between the freeze-dried microcapsules, they easily rehydrated in an aqueous medium and rapidly reassumed their original appearance, as also described by T.A. Comunian et al. [55].

3.4. Determination of Encapsulation Efficiency and Loading Capacity by UV Spectroscopy

To determine the encapsulation efficiency, UV–visible spectroscopic measurements were undertaken. At first, the UV-VIS spectrum of the crude essential oil was recorded at appropriate dilution (Figure 3). The recorded spectrum shows a well-distinguished absorption maxima at 603 nm which can be attributed to the blue-colored chamazulene. Thus, further measurements were performed at this wavelength, and concentrations were determined using a calibration curve.

The calibration diagram was constructed using the concentrations and measured absorbances of six different alcoholic solutions of AMO, ranging from 1 to 10 mg/mL. The resulting equation, $y = 0.0492\ X - 0.0033$ with $R^2 = 0.9993$, demonstrates a high linear correlation between AMO concentrations and absorbances at 603 nm.

The absorbances of the obtained freeze-dried microcapsules dissolved in ethanol were also measured. The AMO-containing microcapsules presented a maximum absorbance at 603 nm, whereas the microcapsules without oil (PL) showed no absorption maximum, indicating that the presence of oil can be detected in the microcapsule solutions.

The encapsulation efficiency (EE) and loading capacity (LC) are presented in Table 6 and should be taken into consideration to determine the efficiency of the microencapsulation process [40,43].

Table 6. Encapsulation efficiency and loading capacity for AMO microcapsules.

Yarrow Essential Oil in Microcapsules	AMO Concentration mg/mL [1]	Concentration of MC Solution mg/mL	Oil Content mg/100 mg MC	Total (Initial) Oil mg/100 mg MC	EE%	LC%
Total oil content	5.961	15	39.74	40.29	87.60	35.29
Surface oil content	0.667	15	4.45	40.29		

[1] Calculated based on the straight-line equation and the measured absorbance values.

The encapsulation efficiency refers to the amount of core material entrapped inside the microcapsules, serving as an important index for evaluating the efficiency of the microencapsulation [59,60]. The EE value obtained in our experiment is relatively high and aligns well with the values reported in the literature obtained through complex coacervation. The ratio of encapsulation efficiency obtained by Rocha-Selmi et al. ranged from 45.15% to 71.70% [58]. For the formulation tested by Ferreira S. and Nicoletti V.R. with the method of complex coacervation, the values of EE varied from 89.7 to 98.7% [40]. The type and composition of the wall material, along with the drying process, play an important role in improving the EE values, which are typically high in complex coacervation involving gelatin in the shell [40,59].

Loading capacity refers to the amount of encapsulated core material relative to the total mass of the microcapsule. Various ranges of loading capacities have been reported in the literature, attributed to differences in the core material, macromolecule species, and the ratio of wall materials. Calderón-Oliver et al. reported encapsulation loadings of nisin and avocado peel extract ranging from 3.05 to 13.59% and 4.58 to 20.54%, respectively [61], while the LC of coacervated black raspberry anthocyanin microcapsules prepared by Shaddel et al. ranged from 29.67 to 38% [62].

3.5. GC—MS Investigation of Microcapsules

The yarrow essential oil composition in its free form and following microencapsulation is presented in Table 7.

Table 7. GC-MS results of components for free and microencapsulated AMO.

No.	Compound	Free AMO Peak%	Microencapsulated AMO Peak%
1.	thujene	1.08	1.12
2.	alpha pinene	4.47	4.68
3.	camphene	0.60	0.51
4.	**sabinene**	**8.31**	**9.05**
5.	**beta pinene**	**8.59**	**10.81**
6.	beta myrcene	0.41	-
7.	alpha terpinene	0.47	-
8.	p cymene	1.55	1.44
9.	D limonene	2.14	1.79
10.	**eucalyptol**	**5.09**	**2.73**
11.	gamma-terpinene	2.18	1.88
12.	artemisia ketone	1.93	1.87
13.	terpinolene	0.32	-
14.	**linalool**	**6.78**	**6.00**
15.	alpha thujone	2.84	3.04
16.	beta thujone	0.46	-
17.	**2-bornanone (camphor)**	**7.84**	**6.68**
18.	1-menthone	0.27	-
19.	endo borneol	1.77	1.75
20.	terpinen 4-ol	1.66	1.16
21.	alpha terpineol	0.42	-
22.	cis dihydrocarvone	0.56	0.43
23.	pulegone	0.30	-
24.	D-carvone	0.60	0.53
25.	**piperitone**	**5.85**	**4.72**
26.	sabinil acetate trans	0.32	-
27.	bornyl acetate	2.68	3.74
28.	thymol	1.31	2.25
29.	diosphenol	0.40	-
30.	carvacrol	1.41	1.27
31.	piperitenone	0.52	-
32.	4-acetyl-1-methylcyclohexene	1.86	0.98
33.	beta bourbonene	0.76	0.71
34.	beta elemene	0.54	0.43
35.	**caryophyllene**	**7.74**	**9.82**
36.	humulene	1.57	1.74
37.	beta farnesene	1.07	0.73
38.	gamma muurolene	0.28	-
39.	**germacrene D**	**6.10**	**7.10**
40.	trans alpha bergamotene	0.63	0.33
41.	cis-γ-bisabolene	0.38	-
42.	cadinene	0.79	0.90
43.	caryophyllene oxide	1.09	1.65
44.	bisabolon oxide A	0.20	0.39
45.	**chamazulene**	**3.80**	**5.14**
	Total	**99.94%**	**97.37%**

In the case of the microencapsulated essential oil, the same major components could be identified, but instead of the initial 45 components, only 33 were present. The loss of some components might be attributed to the microencapsulation technology applied which comprises an emulsification step of essential oil in the gelatin solution performed at approx.

50 °C as well as the drying phase, which is accomplished in reduced pressure conditions, during which some highly volatile components could be lost.

3.6. FT-IR Analysis of Microcapsules

The FTIR spectrum of microencapsulated AMO and the comparison among wavenumbers of FTIR spectra related to the wall materials and unencapsulated core material are shown in Figure 8.

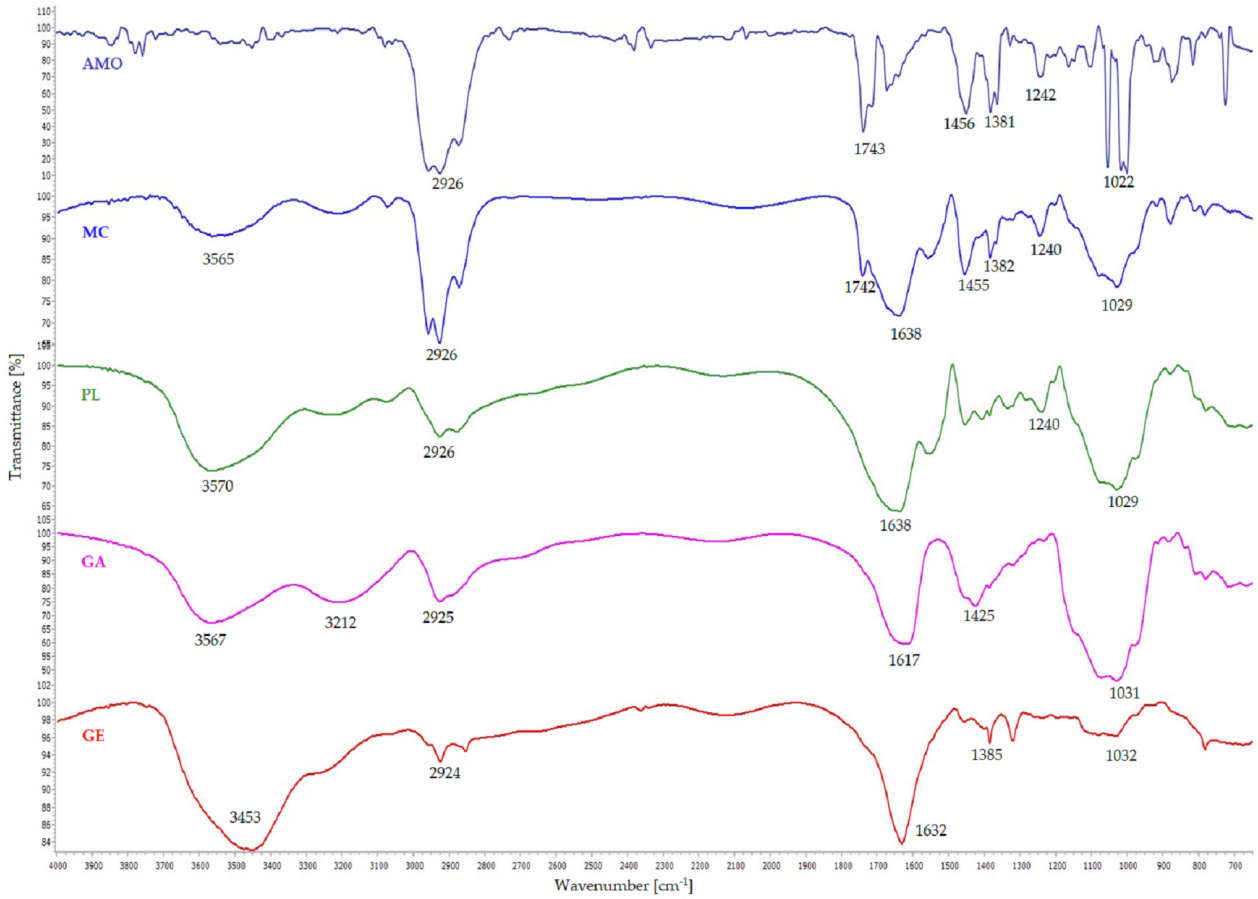

Figure 8. The FT-IR spectrum of yarrow essential oil (AMO), essential oil containing microcapsule (MC), unloaded microcapsule (PL), arabic gum (GA), and gelatin (GE).

The peaks observed in the FT-IR spectrum (Figure 8: AMO) of yarrow essential oil at 2958 cm^{-1}, 2926 cm^{-1}, and 2870 cm^{-1} fall within the range of C-H stretching vibrations, typically associated with aliphatic hydrocarbons, indicating the presence of methylene ($-CH_2-$) and methyl ($-CH_3$) groups. The peaks at 1743 cm^{-1}, 1735 cm^{-1}, and 1712 cm^{-1} correspond to carbonyl (C=O) stretching vibrations, characteristic of ester and ketone functional groups. Wavenumbers 1456 cm^{-1} and 1448 cm^{-1} correspond to C-H bending vibrations (scissoring) in alkanes, while 1381 cm^{-1}, 1367 cm^{-1} and 1362 cm^{-1} indicate C-H bending vibrations (wagging and twisting) in methyl ($–CH_3$) groups. The peaks at 1022 cm^{-1} and 1039 cm^{-1} are due to C–O stretching vibration commonly found in alcohols, ethers, and esters. The peak at 875 cm^{-1}, located in the fingerprint region, could be associated with out-of-plane bending vibrations of C-H bonds, often seen in aromatic compounds or other complex structures [35,63,64].

These interpretations suggest that yarrow essential oil contains a variety of functional groups corresponding to the diversity of terpenes and terpenoids, including saturated and unsaturated aliphatic hydrocarbons (alpha and beta-pinene, sabinene esters, caryophyllene, germacrene D, chamazulene, gamma-terpinene, D-limonene, etc.), ketones (2-bornanone, piperitone, alpha thujone, artemisia ketone, 4-acetyl-1-methylcyclohexene, etc.), alcohols

(linalool, endo borneol, terpinene 4-ol, etc.), ethers (e.g., eucalyptol, caryophyllene oxide), esthers (e.g., bornyl acetate), and aromatic compounds (e.g., p-cymene, carvacrol, thymol).

Arabic gum (GA, also known as gum acacia) is a complex mixture of polysaccharides and glycoproteins. The backbone of arabic gum is mainly composed of 1,3-linked β-D-galactopyranosyl units, with side chains of 1,3-linked β-D-galactopyranosyl units joined to it by 1,6-links. Both main chains and side chains have α-L-arabinofuranosyl, α-L-rhamnopyranosyl, β-D-glucuronopyranosyl and 4-O-methyl-β-D-glucuronopyranosyl units attached. Arabic gum also contains a small proportion of protein (about 1–2%), which is covalently linked to the polysaccharide part. This component is important for the emulsifying properties of the gum [63].

The FT-IR spectrum of gum arabic (Figure 8: GA) is characterized by a strong absorption band at 3567 cm^{-1}, attributed to the –OH stretching vibration, indicative of free or hydrogen-bonded hydroxyl groups associated with the polysaccharide structure. The peak at 3212 cm^{-1} corresponds to the stretching vibrations of N-H bonds, likely due to the protein component of arabic gum or amino acids present in its glycoprotein structure. A weaker peak at 2925 cm^{-1}, characteristic of C-H stretching vibrations in alkyl groups, suggests the presence of hydrocarbon chains within the polysaccharide structure. Additionally, peaks at 1617 cm^{-1} and 1425 cm^{-1} represent asymmetrical and symmetrical stretching vibrations of the carboxylate groups ($–COO^-$), mainly attributed to glucuronic acid units. The strong absorption band at 1031 cm^{-1} corresponds to the asymmetric stretching vibration of –C-O-C and –C-O, which are prevalent in polysaccharides, indicating glycosidic linkages and hydroxyl groups in arabic gum [35,59,64–66].

Gelatin is a polypeptide derived from collagen, primarily composed of the amino acids glycine, proline, hydroxyproline, and glutamic acid [39,62]. The FT-IR spectrum of gelatin (Figure 8: GE) shows a broad peak at 3453 cm^{-1} that reflects the combined contributions of functional groups characteristic of gelatin's complex structure, such as the N-H stretching of amide bonds and $–NH_2$ groups [67,68] and O-H stretching vibrations from hydroxyl groups in amino acid side chains [68]. The peak at 2924 cm^{-1} is due to stretching vibrations of C-H bonds in the aliphatic chains of the amino acid residues, while the one observed at 1385 cm^{-1} is associated with the bending vibrations of C-H bonds in methyl groups [59], indicating the presence of amino acids with methyl-containing side chains. The prominent peak at 1632 cm^{-1} is primarily due to the C=O stretching vibrations of the amide groups in the protein backbone, a characteristic feature of proteins and polypeptides that reflect the peptide bond structure. Lastly, the peak at 1032 cm^{-1} can be attributed to the C-N stretching vibrations of amine groups or the C-O stretching of hydroxyl groups, indicative of the complex structure of amino acid residues and peptide bonds in gelatin [64–66].

During complex coacervation, the free negatively charged carboxylic groups of polysaccharides are expected to interact with the positively charged amino groups of proteins, forming complexes. Figure 8 (PL) shows the FT-IR spectrum of the coacervates, which contains the characteristic peaks of both GA and GE, such as at 3570 cm^{-1}, 2926 cm^{-1}, and a broader peak at 1638 cm^{-1}, which arises from the overlap and slight shift of the GE peak at 1632 cm^{-1} and the GA peak at 1617 cm^{-1}. However, the characteristic peak of the GA spectrum at 1425 cm^{-1} was absent. Similar observations have been reported by other authors for GA—GE coacervates and attributed to the involvement of GA's carboxylic groups in electrostatic interactions with the amino groups of the protein. The appearance of new peaks at 1240 cm^{-1} and 1029 cm^{-1} indicates the presence of N-H groups that can form hydrogen bonds and participate in electrostatic interactions when protonated (NH_3^+) and C-O stretching in arabic gum, supporting the presence of carboxylate groups (COO^-) contributing to negative charges [65].

To investigate the intermolecular interactions between the wall materials and the core material, the spectrum of AMO-loaded microcapsules (Figure 8: MC) was compared with the FTIR spectrum of the essential oil (Figure 8: AMO) and that of unloaded microcapsules (Figure 8: PL). The spectrum of the AMO-containing microcapsules exhibits the same characteristic peaks as the essential-oil-free microcapsules (PL), except for a more intense

peak at 2926 cm^{-1} and the appearance of a new peak at 1450 cm^{-1}, both associated with the C-H stretching and bending vibrations in the aliphatic hydrocarbons found in the composition of the essential oil. These findings suggest that the essential oil was successfully encapsulated and there was no significant interaction between AMO and wall materials [64,66].

3.7. Thermal Analysis of Microcapsules

The DSC thermograms for wall materials, as well as for the blank and AMO-loaded microcapsules, are shown in Figure 9.

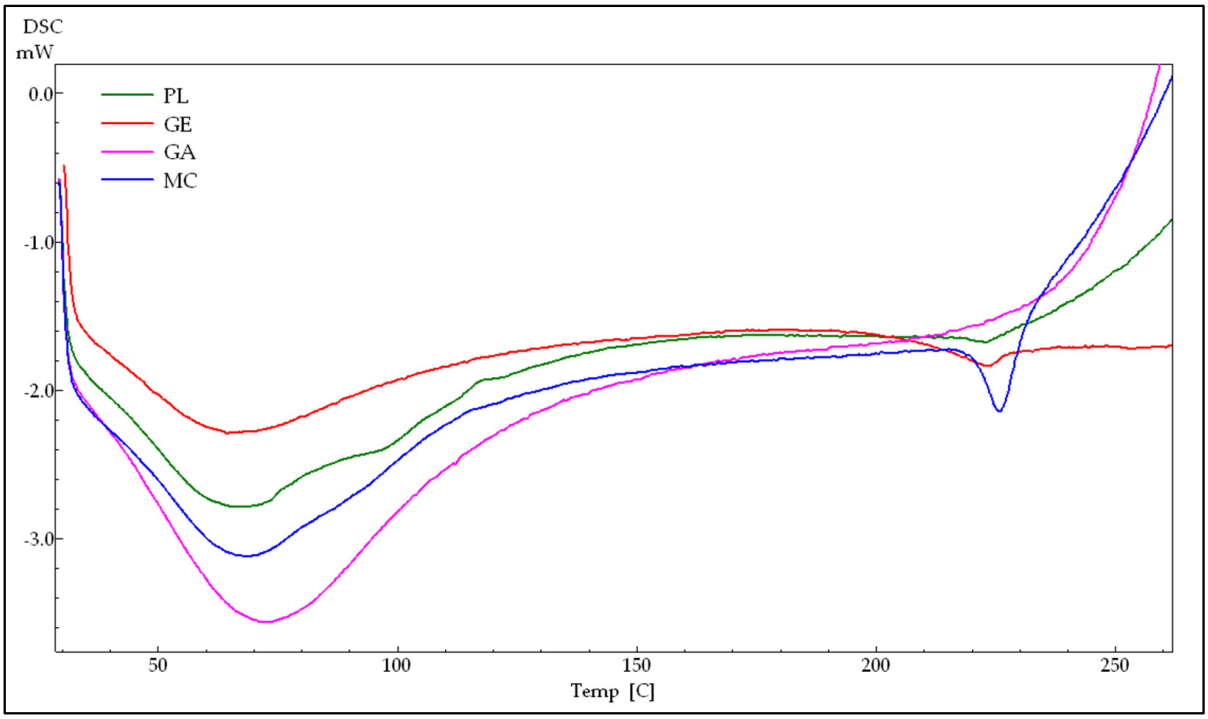

Figure 9. The DSC curves of gelatin (GE), arabic gum (GA), AMO-containing microcapsules (MC) and unloaded microcapsules (PL).

The thermogram of GE (Figure 9: GE) presents an endothermic peak at 64.36 °C, which is associated with water loss overlapping with denaturation [41,65]. According to Rahman et al., an endothermic phenomenon during denaturation is largely attributed to the disruption of hydrogen bonds, leading to protein unfolding, with the denaturation temperature reflecting the thermal stability of proteins [69]. Another peak at 222.85 °C is attributed to the melting of the crystalline fraction and thermal degradation [70]. For GA samples (Figure 9: GA), the broad endothermic peak occurs at 67.89 °C.

Similar endothermic events have been reported by other researchers across a wide temperature range—for GE at 70.96 °C [65] and 62 °C [71], and for GA at 69.87 °C [65], 65 °C [71], 63.31 °C [62], ~75 °C [72], 79.3 °C [73], and 100–150 °C [74]—all of which are attributed to water loss. Given the fact that both GE and GA are natural products, the variations in these values can be attributed to differences in sample composition, moisture content, degree of purity, and storage conditions [65,69,72].

Regarding the microcapsules (Figure 9), the main endothermic peaks are observed at 67.89 °C and 68.13 °C for the PL and MC, respectively. These temperatures are higher than that of pure gelatin (64.36 °C), which is consistent with the results reported for other protein–polysaccharide systems. In these systems, the denaturation temperature of the protein in the coacervates was found to be higher than that of the pure protein, indicating that coacervates provide greater thermal stability [41,65,71,75–77]. The elevated temperature observed for the coacervates suggests enhanced thermal stability compared to the pure

protein and indicates their potential use as wall materials for the encapsulation of thermally sensitive core materials [77].

The DSC thermograms of blank microcapsules displayed a minor endothermic peak at 222.85 °C, corresponding to the melting of the crystalline fraction and thermal degradation of the GE component, while the AMO-loaded microcapsules exhibited a sharp endothermic peak at a higher temperature (225.85 °C). The observation that encapsulating essential oil in gum arabic/gelatin microcapsules shifts the endothermic peaks to higher temperatures and increases the energy required for denaturation and melting, compared to the unloaded microcapsules, suggests changes vs. the PL and interactions between the wall and core materials [41,65,76].

4. Conclusions

Yarrow essential oil that was obtained by steam distillation from plant material brought into cultivation from the spontaneous flora presented chemical profiles with much higher chamazulene (21.97%, 25.37%) and germacrene D (21.28%, 21.13%) levels in two consecutive years compared to commercial samples from two different sources. These results aligned best with data from the literature for essential oil from the western Romanian region. Taking into consideration the diversity in compositions described as well as possible synergism between components, further research work would be required for the assessment of the relationship between the chemical profile and biological activity.

Core–shell-type microcapsules with an average particle size of 47 µm and a polynucleated core containing yarrow essential oil were successfully obtained by complex coacervation technology and transformed into solid-state material by consecutive freeze-drying. SEM images of the freeze-dried form revealed a loose, sponge-like structure with interconnected lyophilized particles by solid bridges.

The technological process was characterized by a high encapsulation efficiency value of approx. 88%.

According to the GC-MS investigation, 33 out of 45 components were present in the microencapsulated yarrow essential oil with the same major compounds.

FT-IR analyses indicated electrostatic interactions between shell components, and that the essential oil was successfully encapsulated and there was no significant interaction between the core and the wall materials. DSC analysis confirmed the successful shell formation surrounding the entrapped essential oil.

Taking into account the multiple biological effects of yarrow essential oil, the authors consider that microencapsulation, due to its protective role and ability to transform material from a liquid state into solid form, is worth being further considered as a potential formulation tool, which might open new application routes for the cosmetic, food, and pharmaceutical industries. Our plans include expanding the plantation size to ensure an adequate amount of raw material for semi-industrial-scale production, which will allow the assessment of self-prepared essential oil as core material and further investigation of the stability and bioactivity of AMO-loaded microcapsules.

Author Contributions: Conceptualization, I.S.-S., E.S. and Z.-I.S.; methodology, I.S.-S.; formal analysis, I.S.-S.; investigation, I.S.-S., C.A., E.M.R., A.-L.G. and B.S.-S.; resources, I.S.-S., C.A., E.M.R., A.-L.G. and B.S.-S.; data curation, I.S.-S.; writing—original draft preparation, I.S.-S.; writing—review and editing, B.S.-S., Z.-I.S. and B.K.; visualization, I.S.-S.; supervision, E.S.; project administration, I.S.-S. and Z.-I.S.; funding acquisition, I.S.-S. and E.S. All authors have read and agreed to the published version of the manuscript.

Funding: This research received no external funding.

Institutional Review Board Statement: Not applicable.

Informed Consent Statement: Not applicable.

Data Availability Statement: The original contributions presented in the study are included in the article; further inquiries can be directed to the corresponding author.

Conflicts of Interest: The authors declare no conflicts of interest.

References

1. Aziz, E.; Badawy, E.; Zheljazkov, V.; Nicola, S.; Fouad, H. Yield and Chemical Composition of Essential Oil of *Achillea Millefolium* L. as Affected by Harvest Time. *Egypt. J. Chem.* **2018**, *62*, 533–540. [CrossRef]
2. Stevanovic, Z.D.; Pljevljakušic, D.; Ristic, M.; Šoštaric, I.; Kresovic, M.; Simic, I.; Vrbnièanin, S. Essential Oil Composition of *Achillea Millefolium* Agg. Populations Collected from Saline Habitats in Serbia. *J. Essent. Oil Bear. Plants* **2015**, *18*, 1343–1352. [CrossRef]
3. Benedek, B.; Rothwangl-Wiltschnigg, K.; Rozema, E.; Gjoncaj, N.; Reznicek, G.; Jurenitsch, J.; Kopp, B.; Glasl, S. Yarrow (*Achillea Millefolium* L. s.l.): Pharmaceutical Quality of Commercial Samples. *Pharmazie* **2008**, *63*, 23–26. [CrossRef] [PubMed]
4. Kindlovits, S.; Cserháti, B.; Inotai, K.; Németh, É.Z. Ontogenetic Variation of Active Agent Content of Yarrow (Achillea Collina Becker). *J. Appl. Res. Med. Aromat. Plants* **2016**, *3*, 52–57. [CrossRef]
5. Karlová, K.; Petříková, K. Variability of the Content of Active Substances during Achillea Collina Rchb. *Alba Ontogenesis. Hortic. Sci.* **2005**, *32*, 17–22. [CrossRef]
6. Orav, A.; Kailas, T.; Ivask, K. Composition of the Essential Oil from *Achillea Millefolium* L. from Estonia. *J. Essent. Oil Res.* **2001**, *13*, 290–294. [CrossRef]
7. European Scientific Cooperative on Phytotherapy. *ESCOP Monographs. The Scientific Foundation for Herbal Medicinal Products*; Online Series—Millefolii Herba (Yarrow); ESCOP: Berlin, Germany, 2021.
8. EDQM Council of Europe. Monograph: Millefolii Herba (07/2014: 1382). In *European Pharmacopoeia (Ph. Eur.)*, 11th ed.; EDQM Council of Europe: Strasbourg, France, 2022; pp. 1781–1782.
9. Kindlovits, S. A mezei cickafark (*Achillea collina* Becker) produkcióját és hatóanyagait befolyásoló tényezők. Ph.D. Thesis, Szent István University, Budapest, Hungary, 2017. [CrossRef]
10. Smelcerovic, A.; Lamshoeft, M.; Radulovic, N.; Ilic, D.; Palic, R. LC-MS Analysis of the Essential Oils of *Achillea Millefolium* and Achillea Crithmifolia. *Chromatographia* **2010**, *71*, 113–116. [CrossRef]
11. Bakun, P.; Czarczynska-Goslinska, B.; Goslinski, T.; Lijewski, S. In Vitro and in Vivo Biological Activities of Azulene Derivatives with Potential Applications in Medicine. *Med. Chem. Res.* **2021**, *30*, 834–846. [CrossRef]
12. Pazouki, L.; Memari, H.R.; Kännaste, A.; Bichele, R.; Niinemets, Ü. Germacrene A Synthase in Yarrow (*Achillea Millefolium*) Is an Enzyme with Mixed Substrate Specificity: Gene Cloning, Functional Characterization and Expression Analysis. *Front. Plant Sci.* **2015**, *6*, 111. [CrossRef]
13. Mustakerova, E.; Todorova, M.; Tsankova, E. Sesquiterpene Lactones from Achillea Collina Becker. *Z. Für Naturforschung C* **2002**, *57*, 568–570. [CrossRef]
14. Li, H.; Li, J.; Liu, M.; Xie, R.; Zang, Y.; Li, J. Phytochemistry Guaianolide Sesquiterpene Lactones from *Achillea Millefolium* L. *Phytochemistry* **2021**, *186*, 112733. [CrossRef] [PubMed]
15. Li, H.; Akber Aisa, H.; Li, J. Germacrane-Type Sesquiterpene Lactones from *Achillea Millefolium* L. and Their Anti-Inflammatory Activity. *Chem. Biodivers.* **2023**, *20*, e202300079. [CrossRef]
16. Gómez de Cedrón, M.; Siles-Sánchez, M.D.L.N.; Martín Hernández, D.; Jaime, L.; Santoyo, S.; Ramírez de Molina, A. Novel Bioactive Extract from Yarrow Obtained by the Supercritical Antisolvent-Assisted Technique Inhibits Lipid Metabolism in Colorectal Cancer. *Front. Bioeng. Biotechnol.* **2024**, *12*, 1256190. [CrossRef] [PubMed]
17. Bocevska, M.; Sovová, H. Supercritical CO_2 Extraction of Essential Oil from Yarrow. *J. Supercrit. Fluids* **2007**, *40*, 360–367. [CrossRef]
18. Villanueva-Bermejo, D.; Zahran, F.; García-Risco, M.R.; Reglero, G.; Fornari, T. Supercritical Fluid Extraction of Bulgarian *Achillea Millefolium*. *J. Supercrit. Fluids* **2017**, *119*, 283–288. [CrossRef]
19. Ivanović, M.; Grujić, D.; Cerar, J.; Islamčević Razboršek, M.; Topalić-Trivunović, L.; Savić, A.; Kočar, D.; Kolar, M. Extraction of Bioactive Metabolites from *Achillea Millefolium* L. with Choline Chloride Based Natural Deep Eutectic Solvents: A Study of the Antioxidant and Antimicrobial Activity. *Antioxidants* **2022**, *11*, 724. [CrossRef]
20. Mohammed, H.A.; Abd-Elraouf, M.; Sulaiman, G.M.; Almahmoud, S.A.; Hamada, F.A.; Khan, R.A.; Hegazy, M.M.; Abd-El-Wahab, M.F.; Kedra, T.A.; Ismail, A. Variability in the Volatile Constituents and Biological Activities of *Achillea Millefolium* L. Essential Oils Obtained from Different Plant Parts and by Different Solvents. *Arab. J. Chem.* **2023**, *16*, 105103. [CrossRef]
21. Gabbanini, S.; Neba, J.N.; Matera, R.; Valgimigli, L. Photochemical and Oxidative Degradation of Chamazulene Contained in Artemisia, Matricaria and Achillea Essential Oils and Setup of Protection Strategies. *Molecules* **2024**, *29*, 2604. [CrossRef]
22. Farasati, B.; Behzad, G.; Khalili, H. *Achillea Millefolium*: Mechanism of Action, Pharmacokinetic, Clinical Drug-Drug Interactions and Tolerability. *Heliyon* **2023**, *9*, e22841. [CrossRef]
23. Applequist, W.L.; Moerman, D.E. Yarrow (*Achillea Millefolium* L.): A Neglected Panacea ? A Review of Ethnobotany, Bioactivity, and Biomedical Research. *Econ. Bot.* **2011**, *65*, 209–225. [CrossRef]

24. Tadić, V.; Arsić, I.; Zvezdanović, J.; Zugić, A.; Cvetković, D.; Pavkov, S. The Estimation of the Traditionally Used Yarrow (*Achillea Millefolium* L. Asteraceae) Oil Extracts with Anti-Inflamatory Potential in Topical Application. *J. Ethnopharmacol.* **2017**, *199*, 138–148. [CrossRef]
25. European Medicines Agency (EMA). *Community Herbal Monograph on Yarrow Herb (Achillea Millefolium L., Herba)*; European Medicines Agency (EMA): Amsterdam, The Netherlands, 2020; Volume EMA/513753.
26. European Medicines Agency (EMA). *Community Herbal Monograph on Yarrow Flower (Achillea Millefolium L., Flos)*; European Medicines Agency (EMA): Amsterdam, The Netherlands, 2019; Volume EMA/165822.
27. Chou, S.T.; Peng, H.Y.; Hsu, J.C.; Lin, C.C.; Shih, Y. *Achillea Millefolium* L. Essential Oil Inhibits LPS-Induced Oxidative Stress and Nitric Oxide Production in RAW 264.7 Macrophages. *Int. J. Mol. Sci.* **2013**, *14*, 12978–12993. [CrossRef] [PubMed]
28. Alomair, M.K.; Alabduladheem, L.S.; Almajed, M.A.; Alobaid, A.A.; Alkhalifah, E.A.R.; Younis, N.S.; Mohamed, M.E. *Achillea Millefolium* Essential Oil Mitigates Peptic Ulcer in Rats through Nrf2/HO-1 Pathway. *Molecules* **2022**, *27*, 908. [CrossRef] [PubMed]
29. Mohamed, M.E.; Elsayed, S.A.; Madkor, H.R.; Eldien, H.M.S.; Mohafez, O.M. Yarrow Oil Ameliorates Ulcerative Colitis in Mice Model via Regulating the NF-κB and PPAR-γ Pathways. *Intest. Res.* **2021**, *19*, 194–205. [CrossRef] [PubMed]
30. Ma, D.; He, J.; He, D. Chamazulene Reverses Osteoarthritic Inflammation through Regulation of Matrix Metalloproteinases (MMPs) and NF-Kβ Pathway in in-Vitro and in-Vivo Models. *Biosci. Biotechnol. Biochem.* **2020**, *84*, 402–410. [CrossRef]
31. Csupor-Löffler, B.; Hajdú, Z.; Zupkó, I.; Réthy, B.; Falkay, G.; Forgo, P.; Hohmann, J. Antiproliferative Effect of Flavonoids and Sesquiterpenoids from *Achillea Millefolium* s.l. on Cultured Human Tumour Cell Lines. *Phyther. Res.* **2009**, *23*, 672–676. [CrossRef]
32. Turek, C.; Stintzing, F.C. Stability of Essential Oils: A Review. *Compr. Rev. Food Sci. Food Saf.* **2013**, *12*, 40–53. [CrossRef]
33. Sousa, V.I.; Parente, J.F.; Marques, J.F.; Forte, M.A.; Tavares, C.J. Microencapsulation of Essential Oils: A Review. *Polymers* **2022**, *14*, 1730. [CrossRef]
34. Arenas-Jal, M.; Suñé-Negre, J.M.; García-Montoya, E. An Overview of Microencapsulation in the Food Industry: Opportunities, Challenges, and Innovations. *Eur. Food Res. Technol.* **2020**, *246*, 1371–1382. [CrossRef]
35. Rakmai, J.; Cheirsilp, B.; Torrado-agrasar, A.; Simal-, J.; Mejuto, J.C.; Torrado-agrasar, A. Encapsulation of Yarrow Essential Oil in Hydroxypropyl-Beta-Cyclodextrin: Physiochemical Characterization and Evaluation of Bio-Efficacies. *CyTA-J. Food* **2017**, *15*, 409–417. [CrossRef]
36. Ahmadi, Z.; Saber, M.; Bagheri, M.; Mahdavinia, G.R. *Achillea Millefolium* Essential Oil and Chitosan Nanocapsules with Enhanced Activity against Tetranychus Urticae. *J. Pest Sci.* **2018**, *91*, 837–848. [CrossRef]
37. Timilsena, Y.P.; Akanbi, T.O.; Khalid, N.; Adhikari, B.; Barrow, C.J. Complex Coacervation: Principles, Mechanisms and Applications in Microencapsulation. *Int. J. Biol. Macromol.* **2019**, *121*, 1276–1286. [CrossRef] [PubMed]
38. Thies, C. Encapsulation by Complex Coacervation. In *Encapsulation and Controlled Release Technologies in Food Systems*; Lakkis, J.M., Ed.; John Wiley & Sons, Inc.: Hoboken, NJ, USA, 2016; pp. 41–77. ISBN 9781118946893.
39. Milano, F.; Masi, A.; Madaghiele, M.; Sannino, A.; Salvatore, L.; Gallo, N. Current Trends in Gelatin-Based Drug Delivery Systems. *Pharmaceutics* **2023**, *15*, 1499. [CrossRef] [PubMed]
40. Ferreira, S.; Nicoletti, V.R. Microencapsulation of Ginger Oil by Complex Coacervation Using Atomization: Effects of Polymer Ratio and Wall Material Concentration. *J. Food Eng.* **2021**, *291*, 110214. [CrossRef]
41. Yang, X.; Gao, N.; Hu, L.; Li, J.; Sun, Y. Development and Evaluation of Novel Microcapsules Containing Poppy-Seed Oil Using Complex Coacervation. *J. Food Eng.* **2015**, *161*, 87–93. [CrossRef]
42. Gonçalves, N.D.; de Lima Pena, F.; Sartoratto, A.; Derlamelina, C.; Duarte, M.C.T.; Antunes, A.E.C.; Prata, A.S. Encapsulated Thyme (*Thymus Vulgaris*) Essential Oil Used as a Natural Preservative in Bakery Product. *Food Res. Int.* **2017**, *96*, 154–160. [CrossRef]
43. Eratte, D.; Wang, B.; Dowling, K.; Barrow, C.J.; Adhikari, B.P. Complex Coacervation with Whey Protein Isolate and Gum Arabic for the Microencapsulation of Omega-3 Rich Tuna Oil. *Food Funct.* **2014**, *5*, 2743–2750. [CrossRef]
44. Khan, M.; Al-Saleem, M.S.M.; Alkhathlan, H.Z. A Detailed Study on Chemical Characterization of Essential Oil Components of Two Plectranthus Species Grown in Saudi Arabia. *J. Saudi Chem. Soc.* **2016**, *20*, 711–721. [CrossRef]
45. Jianu, C.; Misca, C. Composition, Antioxidant and Antimicrobial Activity of the Essential Oil of Achillea Collina Becker Growing Wild in Western Romania. *Hem. Ind.* **2014**, *69*, 381–386. [CrossRef]
46. Iuliana Costescu, C.; Rădoi, B.P.; Hădărugă, N.G.; Gruia, A.T.; Riviş, A.; Pârvu, D.; David, I.; Hădărugă, D.I. Obtaining and Characterization of *Achillea Millefolium* L. Extracts. *J. Agroaliment. Process. Technol.* **2014**, *20*, 142–149.
47. Yildirim, B.; Ekici, K.; Kocak, M.Z. Essential oil composition of yarrow species (*Achillea millefolium* L. and *Achillea wilhelmsii* L.): Antioxidant and antibacterial activities. *Stud. UBB Chem.* **2023**, *68*, 145–157. [CrossRef]
48. Abdossi, V.; Kazemi, M. Bioactivities of *Achillea Millefolium* Essential Oil and Its Main Terpenes from Iran. *Int. J. Food Prop.* **2015**, *19*, 1798–1808. [CrossRef]
49. Farhadi, N.; Babaei, K.; Farsaraei, S.; Moghaddam, M.; Ghasemi Pirbalouti, A. Changes in Essential Oil Compositions, Total Phenol, Flavonoids and Antioxidant Capacity of *Achillea Millefolium* at Different Growth Stages. *Ind. Crop. Prod.* **2020**, *152*, 112570. [CrossRef]
50. Cristina Figueiredo, A.; Barroso, J.G.; Salomé, M.; Pais, S.; Scheffer, J.J.C. Composition of the Essential Oils from Two Populations of *Achillea Millefolium* L Ssp. Millefolium. *J. Chromatogr. Sci.* **1992**, *30*, 392–395. [CrossRef]

51. Daniel, P.S.; Lourenço, E.L.B.; da Cruz, R.M.S.; De Souza Gonçalves, C.H.; Das Almas, L.R.M.; Hoscheid, J.; da Silva, C.; Jacomassi, E.; Brum, L.; Alberton, O. Composition and Antimicrobial Activity of Essential Oil of Yarrow (*Achillea Millefolium* L.). *Aust. J. Crop Sci.* **2020**, *14*, 545–550. [CrossRef]
52. Verma, R.S.; Joshi, N.; Padalia, R.C.; Goswami, P.; Singh, V.R.; Chauhan, A.; Verma, S.K.; Iqbal, H.; Verma, R.K.; Chanda, D.; et al. Chemical Composition and Allelopathic, Antibacterial, Antifungal and in Vitro Acetylcholinesterase Inhibitory Activities of Yarrow (*Achillea Millefolium* L.) Native to India. *Ind. Crop. Prod.* **2017**, *104*, 144–155. [CrossRef]
53. Konarska, A.; Weryszko-Chmielewska, E.; Sulborska-Różycka, A.; Kiełtyka-Dadasiewicz, A.; Dmitruk, M.; Gorzel, M. Herb and Flowers of *Achillea Millefolium* Subsp. *Millefolium L.: Structure and Histochemistry of Secretory Tissues and Phytochemistry of Essential Oils. Molecules* **2023**, *28*, 7791. [CrossRef]
54. El-Kalamouni, C.; Venskutonis, P.; Zebib, B.; Merah, O.; Raynaud, C.; Talou, T. Antioxidant and Antimicrobial Activities of the Essential Oil of *Achillea Millefolium* L. *Grown in France. Medicines* **2017**, *4*, 30. [CrossRef]
55. Comunian, T.A.; Thomazini, M.; Alves, A.J.G.; de Matos Junior, F.E.; de Carvalho Balieiro, J.C.; Favaro-Trindade, C.S. Microencapsulation of Ascorbic Acid by Complex Coacervation: Protection and Controlled Release. *Food Res. Int.* **2013**, *52*, 373–379. [CrossRef]
56. Alvim, I.D.; Grosso, C.R.F. Microparticles Obtained by Complex Coacervation: Influence of the Type of Reticulation and the Drying Process on the Release of the Core Material. *Ciência Tecnol. Aliment.* **2010**, *30*, 1069–1076. [CrossRef]
57. Saravanan, M.; Rao, K.P. Pectin–Gelatin and Alginate–Gelatin Complex Coacervation for Controlled Drug Delivery: Influence of Anionic Polysaccharides and Drugs Being Encapsulated on Physicochemical Properties of Microcapsules. *Carbohydr. Polym.* **2010**, *80*, 808–816. [CrossRef]
58. Rocha-Selmi, G.A.; Bozza, F.T.; Thomazini, M.; Bolini, H.M.A.; Fávaro-Trindade, C.S. Microencapsulation of Aspartame by Double Emulsion Followed by Complex Coacervation to Provide Protection and Prolong Sweetness. *Food Chem.* **2013**, *139*, 72–78. [CrossRef] [PubMed]
59. Zhang, R.; Huang, L.; Xiong, X.; Qian, M.C.; Ji, H. Preparation and Release Mechanism of Lavender Oil Microcapsules with Different Combinations of Coating Materials. *Flavour Fragr. J.* **2020**, *35*, 157–166. [CrossRef]
60. Baghi, F.; Ghnimi, S.; Dumas, E.; Gharsallaoui, A. Microencapsulation of Antimicrobial Trans-Cinnamaldehyde: Effect of Emulsifier Type, PH, and Drying Technique. *Appl. Sci.* **2023**, *13*, 6184. [CrossRef]
61. Calderón-Oliver, M.; Pedroza-Islas, R.; Escalona-Buendía, H.B.; Pedraza-Chaverri, J.; Ponce-Alquicira, E. Comparative Study of the Microencapsulation by Complex Coacervation of Nisin in Combination with an Avocado Antioxidant Extract. *Food Hydrocoll.* **2017**, *62*, 49–57. [CrossRef]
62. Shaddel, R.; Hesari, J.; Azadmard-Damirchi, S.; Hamishehkar, H.; Fathi-Achachlouei, B.; Huang, Q. Use of Gelatin and Gum Arabic for Encapsulation of Black Raspberry Anthocyanins by Complex Coacervation. *Int. J. Biol. Macromol.* **2018**, *107*, 1800–1810. [CrossRef]
63. Musa, H.H.; Ahmed, A.A.; Musa, T.H. *Chemistry, Biological, and Pharmacological Properties of Gum Arabic*; Springer: Cham, Switzerland, 2019; pp. 797–814.
64. Larkin, P.J. IR and Raman Spectra–Structure Correlations: Characteristic Group Frequencies. *Infrared Raman Spectrosc.* **2018**, 85–134. [CrossRef]
65. Rousi, Z.; Malhiac, C.; Fatouros, D.G.; Paraskevopoulou, A. Complex Coacervates Formation between Gelatin and Gum Arabic with Different Arabinogalactan Protein Fraction Content and Their Characterization. *Food Hydrocoll.* **2019**, *96*, 577–588. [CrossRef]
66. Stuart, B.H. Infrared Spectroscopy: Fundamentals and Applications. In *Analytical Techniques in the Sciences*; John Wiley & Sons, Inc.: Hoboken, NJ, USA, 2004; pp. 71–80. ISBN 9780470854273.
67. Long, Y.; Song, K.; York, D.; Zhang, Z.; Preece, J.A. Composite Microcapsules with Enhanced Mechanical Stability and Reduced Active Ingredient Leakage. *Particuology* **2016**, *26*, 40–46. [CrossRef]
68. Santos, M.G.; Bozza, F.T.; Thomazini, M.; Favaro-Trindade, C.S. Microencapsulation of Xylitol by Double Emulsion Followed by Complex Coacervation. *Food Chem.* **2015**, *171*, 32–39. [CrossRef]
69. Rahman, M.S.; Al-Saidi, G.; Guizani, N.; Abdullah, A. Development of State Diagram of Bovine Gelatin by Measuring Thermal Characteristics Using Differential Scanning Calorimetry (DSC) and Cooling Curve Method. *Thermochim. Acta* **2010**, *509*, 111–119. [CrossRef]
70. Ang, L.; Darwis, Y.; Por, L.; Yam, M. Microencapsulation Curcuminoids for Effective Delivery in Pharmaceutical Application. *Pharmaceutics* **2019**, *11*, 451. [CrossRef]
71. Yüksel, A.; Şahin-Yeşilçubuk, N. Encapsulation of Structured Lipids Containing Medium- and Long Chain Fatty Acids by Complex Coacervation of Gelatin and Gum Arabic. *J. Food Process Eng.* **2018**, *41*, e12907. [CrossRef]
72. Outuki, P.M.; de Francisco, L.M.B.; Hoscheid, J.; Bonifácio, K.L.; Barbosa, D.S.; Cardoso, M.L.C. Development of Arabic and Xanthan Gum Microparticles Loaded with an Extract of Eschweilera Nana Miers Leaves with Antioxidant Capacity. *Colloids Surfaces A Physicochem. Eng. Asp.* **2016**, *499*, 103–112. [CrossRef]
73. Singh, B.; Sharma, S.; Dhiman, A. Acacia Gum Polysaccharide Based Hydrogel Wound Dressings: Synthesis, Characterization, Drug Delivery and Biomedical Properties. *Carbohydr. Polym.* **2017**, *165*, 294–303. [CrossRef]
74. Daoub, R.M.A.; Elmubarak, A.H.; Misran, M.; Hassan, E.A.; Osman, M.E. Characterization and Functional Properties of Some Natural Acacia Gums. *J. Saudi Soc. Agric. Sci.* **2018**, *17*, 241–249. [CrossRef]

75. Duhoranimana, E.; Karangwa, E.; Lai, L.; Xu, X.; Yu, J.; Xia, S.; Zhang, X.; Muhoza, B.; Habinshuti, I. Effect of Sodium Carboxymethyl Cellulose on Complex Coacervates Formation with Gelatin: Coacervates Characterization, Stabilization and Formation Mechanism. *Food Hydrocoll.* **2017**, *69*, 111–120. [CrossRef]
76. Huang, G.Q.; Sun, Y.T.; Xiao, J.X.; Yang, J. Complex Coacervation of Soybean Protein Isolate and Chitosan. *Food Chem.* **2012**, *135*, 534–539. [CrossRef] [PubMed]
77. Timilsena, Y.P.; Wang, B.; Adhikari, R.; Adhikari, B. Preparation and Characterization of Chia Seed Protein Isolate-Chia Seed Gum Complex Coacervates. *Food Hydrocoll.* **2015**, *52*, 554–563. [CrossRef]